OUKA
The University of Osaka
Institutional Knowledge Archive

Title	Fatigue Crack Propagation in Steels under Random Loading
Author(s)	Fukuda, Shuichi; Kitagawa, Hideo
Citation	Transactions of JWRI. 1977, 6(2), p. 185-192
Version Type	VoR
URL	https://doi.org/10.18910/7218
rights	
Note	

The University of Osaka Institutional Knowledge Archive : OUKA

https://ir.library.osaka-u.ac.jp/

The University of Osaka

Fatigue Crack Propagation in Steels under Random Loading†

Shuichi FUKUDA* and Hideo KITAGAWA**

Abstract

This investigation was carried out in order to clarify experimentally fatigue crack propagation in steels under stationary random fully reversed tension-compression loading. Sine wave loads and random loads with different power spectra were applied to S20C-equivalent and S35C-equivalent steel specimens under displacement-controlled and load-controlled loading. The fundamental properties of fatigue crack propagation, the effect of power spectra, and the threshold for fatigue crack propagation in steels under random loading were clarified.

1. Introduction

This paper is an experimental research work which studied fatigue crack propagation in steels under random loading on the basis of linear fracture mechanics. As fatigue crack propagation data in steels under random loading is quite scarce, it was studied experimentally and the results which were obtained under different loading conditions and by different geometries were presented in a unified manner using linear fracture mechanics. The effects of power spectral density of the random load upon fatigue crack propagation and the threshold condition for a fatigue crack to grow under random loading were also made clear.

Since the research of fatigue crack propagation under random loading is originally aimed at practical applications, the results must be applicable not only to any form of service loads, but also to any structural members of any geometry. Thus, the experimental results of two series of tests; displacement-controlled tests and load-controlled tests, were presented in a unified manner using stress intensity factor, because the stress intensity factor K can incorporate the effect of loading conditions and specimen geometries. So far as fatigue crack propagation under random loading is concerned, although there are many results on airplane materials such as aluminum alloys, results on steels which are extensively used in various industrial fields are quite few[1),2)]. Further, although the threshold condition K_{th} for sinusoidal loading has been obtained by many investigators for various kinds of materials, the K_{th} for random loading has not, at least to the authors' knowledge, been studied up to now. Three kinds of power spectra were applied in this study; two different power spectra were applied in the displacement-controlled tests, and a power spectrum of another kind was applied in the load-controlled tests. These three power spectra were generated simulating the power spectra of the automobile service loads.

2. Experimental setups and procedure

The same electro-dynamic type fatigue testing machine was used for both displacement-controlled tests and load-controlled tests. The schematic of the testing setup is shown in **Fig. 1.** In both series of tests, fully reversed loads were applied and the specimens were tested in "as manufactured" condition without heat treatment. The final surface finishing is performed by buffing with chromium oxide. The crack length was measured from the developed close-up films by magnifying them 20 times on a projector. These films were photographed at regular intervals using 250 shot motor-driven camera. The number of cycles was calculated from the elapsed time of a clock which image was focused on a film by utilizing the optical setup of a convex lens and a plane mirror. The rms values σ_{rms} of the instantaneous values of the

† Received on October 31, 1977

* Research Instructor

** Professor, Institute of Industrial Science, University of Tokyo

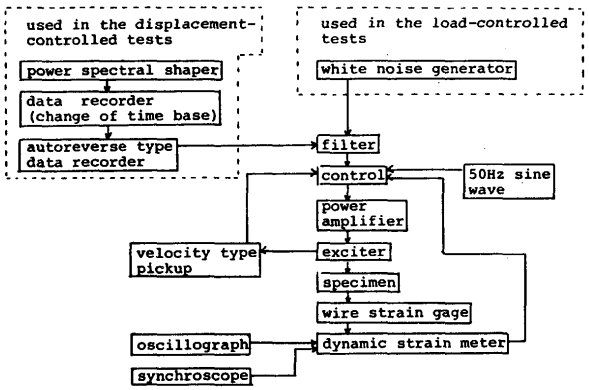

Fig. 1 Schematic of electrodynamic fatigue testing setup

random loads were computed by reading the visigraph records on a tracer.

2.1 Displacement-controlled tests

In this series of tests, displacement-controlled fully reversed tension-compression load was applied to a thin steel sheet specimen by making use of the bending of a composite beam. Three kinds of loads were applied; sine wave load, random load A, and random load B. The material tested was KTH38D cold-rolled steel sheet of Kawasaki Steel Coorporation and its chemical composition and mechanical properties were shown in **Table 2.** The geometry and the size of the specimen is shown in **Fig. 3.**

2.1.1 *Displacement-controlled tension-compression testing setup utilizing the bending of a composite beam*

In this series of tests, tension-compression load was applied to a thin steel sheet by utilizing the outermost bending fiber stress of a composite beam; crack growth in an approximate uni-axial tension-compression stress state was observed by sticking thin steel sheet specimens on the top and bottom surfaces of a thick aluminum base just in the form of sandwich panels. These steel sheets are so thin that their stress gradients can be ignored and that their stress distributions can be re-

Table 1 Comparison of displacement-controlled tests and load-controlled tests

	displacement-controlled tests		load-controlled tests
sine wave	same oscillator was used (50Hz)		
random load	signals with desired power spectra generated by a power spectral shaper were recorded on an autoreverse data recorder after the change of time base, then it was used as an external input		white noise generated by a thyratron was bandpassed through 30-50 Hz filters (25 dB/oct) and it was used as an external input
random load	A	B	C
N_0	38.9	23.3	38.4
N_p	39.9	26.6	40.7
N_0/N_p	0.98	0.88	0.94
C.R.	2.8	3.2	4.2
Power spectra	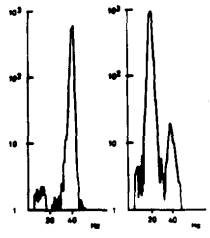		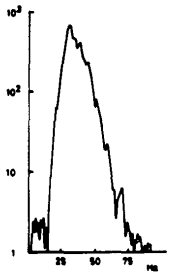

N_0=number of zero crossings per unit time (sec)

N_p=number of peaks per unit time (sec)

C.R.=clipping ratio

Table 2 Chemical composition and mechanical properties of displacement-controlled test specimen

C	Si	Mn	P	S	tensile strength	elongation	hardness H_v (200)
0.19	trace	0.44	0.008	0.021	44 kg/mm^2	35%	148

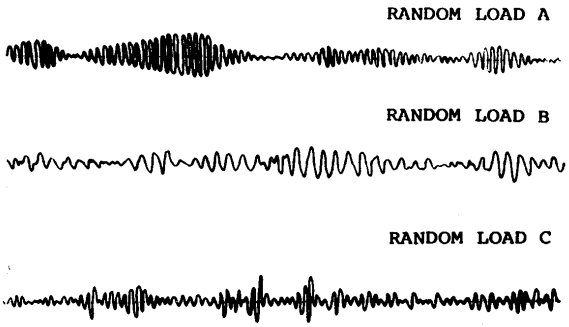

Fig. 2 Random loads applied

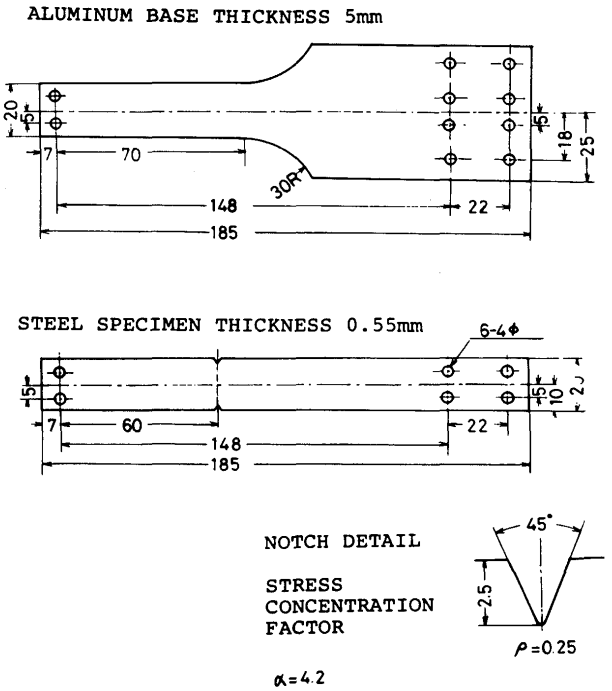

Fig. 3 Size and geometry of the specimen used in displacement-controlled tests

garded as uniform along the thickness. As a high strength aluminum alloy was used for a base and mild steel was used for the test specimen, the stress produced in the steel specimen was three times that of an aluminum base since the Young's modulus of a steel is three times that of an aluminum, therefore, only steel specimen breaks. Under the mere bending load, the accurate measurement of crack growth is quite difficult because a crack extends into the thickness direction and the analysis of the stress field at the crack tip is also difficult in the case of plane bending. But these problems can be eliminated by the adoption of the above technique. In an ordinary one-body notched specimen, the rigidity of the test specimen decreases with crack extension so that the frequency response of the testing system changes. Therefore, the test using an ordinary one-body notched specimen brings about various difficult problems as a control system especially in the case of a random load test. By adopting the above mentioned technique, however, the rigidity of the testing system does not decrease with crack extension and the change of the frequency response is negligible so that its control is easy. The schematic of this setup is shown in **Fig. 4.** One end of the cantilever composite beam which consists of steel sheet specimens and an aluminum base is fixed and another end of the beam is connected to the axle of an exciter. The deflection of the beam is proportional to the voltage of the input signal. Therefore, this test is a displacement-controlled test. The true notched steel sheet specimen was stuck on the top of the base and the dummy unnotched sheet specimen of the same geometry and size was attached on the bottom. The 20 mm length part shown as unhatched in Fig. 4 was not stuck to the base to avoid the effect of base constraint on the stress concentration of steel sheet specimen. The length of this unhatched part was determined by the condition that the sheet specimen does not buckle in compression. The stress value of the tested part was

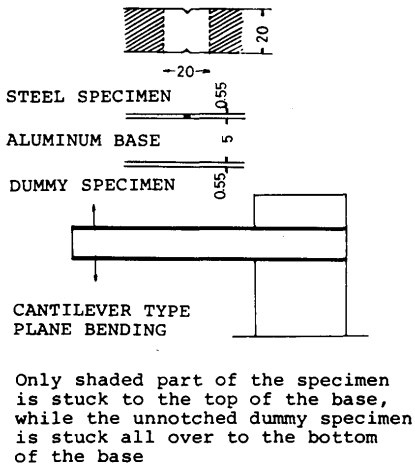

Fig. 4 Displacement-controlled tension-compression test utilizing the bending of a composite beam

evaluated by attaching the wire strain gage to the 50 mm width part of the aluminum base.

2.1.2 *Application of random loads*

In the displacement-controlled tests, two kinds of random loads were applied; random load A with unimodal power spectrum and random load B with bimodal power spectrum. The irregularity factor N_0/N_p which is often used as a simple index for the degree of irregularity of a random load although its accuracy is not good, is 0.98 for random load A and 0.88 for random load B. The power spectra and other fundamental parameters such as N_o/N_p of the random loads applied are shown in Table 1. The random load with a desired power spectrum was generated using a power spectral shaper which consists of 40 parallel narrow bandpass filters and the same number of feedback circuits. The output signal of the shaper was then recorded on a FM data recorder and to change the time base, it was re-recorded on an auto-reverse type FM data recorder at the recording speed of 9.5 cm/s. The length of the record is approximately 45 minutes one way, i.e., 90 minutes both ways. The output signal of this auto-reverse data recorder was then passed through a bandpass filter of 8–50 Hz and was used as an input signal to the electrodynamic fatigue testing machine. The type of the autoreverse data recorder was such that as soon as the metal foil attached to the magnetic tape contacts the sensor, and the circuit is cut short, the circuit works so that the output signal becomes zero and it is kept zero for approximately 10 seconds until the mechanism stabilizes after the servomotor reverses. If the signal is recorded at the tape speed of 9.5 cm/s, one hour's recording is possible for one way so that 'no load' period takes place only at the rate of 10 seconds per hour. The autoreverse type has the advantage of (1) there is no possibility of impulsive loading due to the connection of the tape, (2) the length of recording time is long. (3) the wear of recording heads and tapes can be reduced.

2.2 Load-controlled tests

In this series of tests, load was magnified 14 times using a lever and fully reversed tension-compression load was applied to a steel sheet specimen. The material tested was S35C-equivalent railroad axle steel. Its chemical composition and mechanical properties are shown in **Table 3.** The size and geometry of the test specimen is shown in **Fig. 5.** Only one kind of random load was generated by the procedure shown in Table 1. Fig. 2 shows the random load C applied.

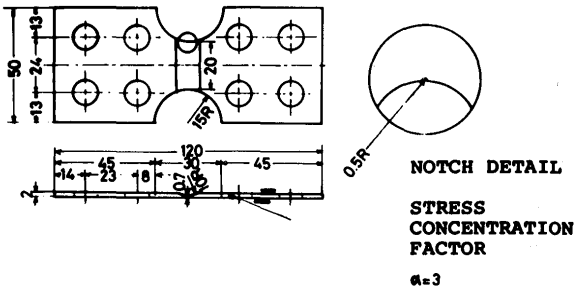

Fig. 5 Size and geometry of the specimen used in load-controlled tests

3. Computation of the stress intensity factor K

3.1 Displacement-controlled tests

In the following, the stress analysis was carried out assuming that the steel sheet specimen was subjected to tension-compression loading because this steel sheet specimen is so thin that its bending stress gradient can be ignored and that stress can be assumed uniformly distributed across the thickness. Once a crack is formed in a thin steel sheet specimen, the redistribution of the load takes place between steel sheets and an aluminum base. Prof. H. Okamura et al. proposed a method for estimating the amount of load decrease considering the change of compliance with crack extension[3]. In the following Okamura's formula,

$$P=P_0/(1+\kappa\frac{\Delta\lambda}{\lambda_0}) \quad (1)$$

Table 3 Chemical composition and mechanical properties of load-controlled test specimen

C	Si	Mn	P	S
0.35	0.30	0.70	0.014	0.014

tensile strength	yield point	elongation	contraction of area	Charpy impact value
56.0	29.7	31.0%	53.9%	9.1 kg-m/cm^2

κ denotes the factor for the degree of constraint, and for full constraint $\kappa=1$. Since the composite beam which consists of steel sheets and an aluminum base is, as one body, subjected to displacement control in this series of tests, the steel sheet specimen can be regarded as being subjected to the displacement-controlled tension-compression load. Therefore, κ was put equal to 1. λ_0 and P_0 is the compliance and load without crack respectively and $\Delta\lambda$ is the change of compliance with crack extension. The $\frac{\Delta\lambda}{\lambda_0}$ value in Eq. (1) can be obtained as follows; in this series of tests, the testing part of a steel sheet specimen and an aluminum base is not stuck and the thickness t of the steel sheet specimen can be regarded as thin enough to be plane stress. From the change of energy when the area of a crack changes by the amount $dA=td(2a)$,

$$\frac{K^2}{E}=\frac{P^2 d\lambda}{2dA} \text{ (plane stress)} \tag{2}$$

As the specimen used in this series of tests is a double-edge-notched specimen with the geometry of (specimen length L)/(specimen width W)=1, O.L. Bowie's solution[4] can be applied if we regard (notch depth+ actual crack length) as crack length. If we denote Bowie's correction factor for Westergaard's equation

$$K=\sigma\sqrt{\pi a}\sqrt{\frac{W}{\pi a}\tan\left(\frac{\pi a}{W}\right)} \tag{3}$$

by $h(a/W)$, then the stress intensity factor K can be obtained as,

$$K=\sigma\sqrt{\pi a}\sqrt{\frac{W}{\pi a}\tan\left(\frac{\pi a}{W}\right)}h\left(\frac{a}{W}\right) \tag{4}$$

Substituting Eq. (4) into Eq. (2), and considering $\sigma=\frac{P}{Wt}$, $\lambda_0=\frac{L}{EtW}$

where E denotes Young's modulus, and integrating Eq. (2) yields,

$$\frac{\Delta\lambda}{\lambda_0}=2\frac{W}{L}\int_0^{2a/W}\tan\left(\frac{\pi a}{W}\right)h^2\left(\frac{a}{W}\right)d\left(\frac{2a}{W}\right) \tag{5}$$

The results of the estimated amount of load decrease in the displacement-controlled tests obtained by Okamura's method and finite element method are shown in **Fig. 6**, together with the experimental results. These results agree quite well.

3.2. Load-controlled tests

As the specimen used in this series of tests can be regarded as being rigidly fixed except at the neighbourhood of notches, the semi-circular notches with $\rho=0.5$ mm act alone as stress raisers. Therefore, in the following analysis, the specimen was assumed as being of uniform thickness and width with $L=10$ mm, and $W=20$ mm. As the specimen is short in length with such a geometry of $L/W=0.5$, the boundary conditions affect the value of the stress intensity factor K. O.L. Bowie[5] gave a solution for a plate with both ends fixed rigidly. The K value Bowie obtained agrees with Westergaard's solution, i.e., Eq. (3) for a wide range of a. Therefore, K is approximated by the Westergaard's solution in this analysis. Further, the appropriateness of the approximation of K by the Westergaard's solution is confirmed using 2-dimensional finite element method by changing the element thicknesses.

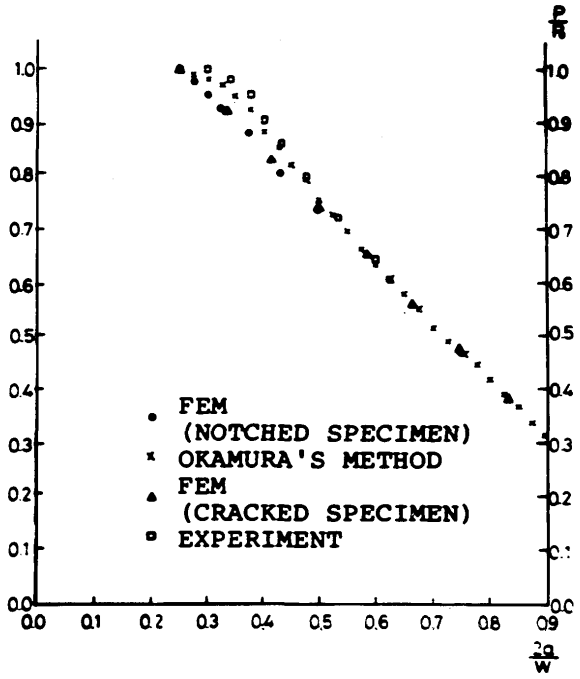

Fig. 6 Load decrease in displacement-controlled tests

4. Experimental results and discussion

4.1 Displacement-controlled tests

The experimental results of sine wave load, random load A, and random load B are shown in **Fig. 7–Fig. 9.** In the case of sine wave load, stress intensity factor is expressed in terms of its stress amplitude and is denoted by K_a. The n value in the expression $d(2a)/dN=CK_a^n$ was obtained as $n=4$ by the least square method. This indicates that the fourth power law holds even in the displacement-controlled tests if the decrease of load is taken into account. In the case of random loading, n is approximately 3.9 for random load A and approximately 3.3 for random load B, if the stress intensity factor is expressed in terms of the instantaneous rms value of the random

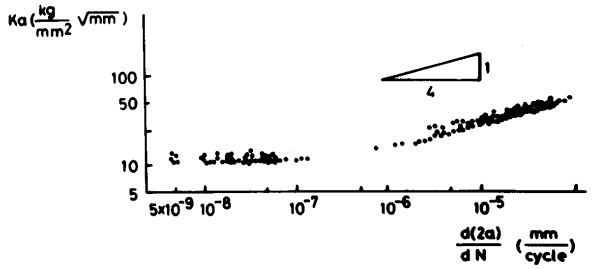

Fig. 7 Results of displacement-controlled sine wave load tests

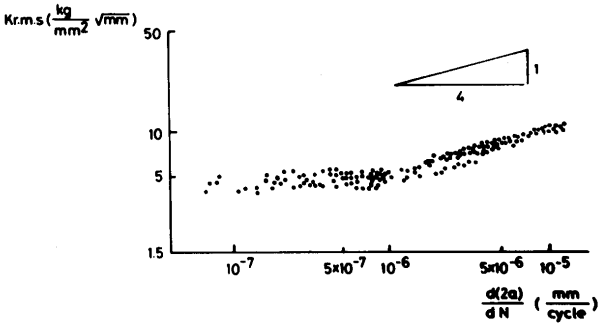

Fig. 8 Results of displacement-controlled random load tests (random load A)

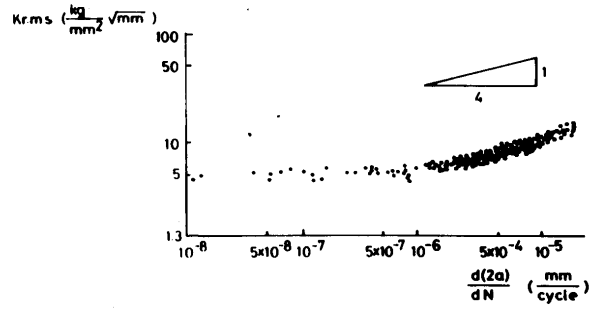

Fig. 9 Results of displacement-controlled random load tests (random load B)

stress. In both cases, n is nearly 4 and there is no appreciable effect of bandwidth. But it is observed, however, that as the bandwidth increases, n shows a tendency, to approach 3. If we take the minimum K level of the flat region in $d(2a)/dN \sim K$ curve as the threshold stress intensity factor K_{th} for crack growth, $(K_a)_{th}$ for sine wave load is approximately 12 kg/mm^2 $\sqrt{\text{mm}}$, and $(K_{rms})_{th}$ for random load is approximately 4 kg/mm$^2\sqrt{\text{mm}}$ either under random load A or under random load B. In the case of random loading, the data in the flat region of $d(2a)/dN \sim K$ curve does not contain the non-propagating crack data but in the case of sine wave loading, the data in the flat region include the non-propagating crack data.

4.2 Load-controlled tests

Experimental results are shown in **Fig. 10.** Stress

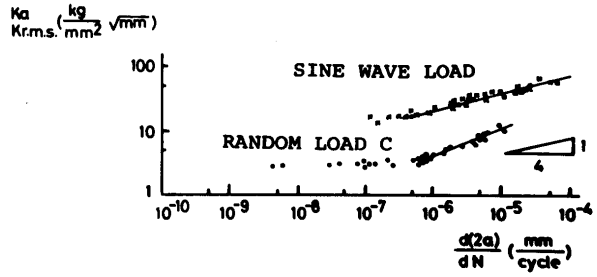

Fig. 10 Results of load-controlled tests

intensity factors are expressed in the form of K_a for sine wave load, and K_{rms} for random load. The n value in the equation $d(2a)/dN=CK^n$ was obtained as approximately 4 for sine wave load, and as approximately 3 for random load. In the case of sine wave load, the data in the flat region does not contain non-propagating data, but in the case of random load, the data in the flat region include non-propagating data. The K_{th} values obtained were $(K_a)_{th}=12$ kg/mm$^2\sqrt{\text{mm}}$ for sine wave load, and $(K_{rms})_{th}=3$ kg/mm$^2\sqrt{\text{mm}}$.

4.3 Comparison of the results of two experiments and discussion

In the case of sine wave load, the C value in the equation $d(2a)/dN=CK_a^4$ was obtained as $C=7.78\times 10^{-12}$ for displacement-controlled tests and $C=6.38\times 10^{-12}$ for load-controlled tests. Kitagawa and Misumi [6] found the relation $\log C=-4.5-n\times 1.74$ between C and n in the equation $d(2a)/dN=CK_a^4$. This relation holds generally for a wide variety of materials. If we put $n=4$, the above equation gives $\log C=-11.46$. The $\log C$ values in these experiments are $\log C=-11.11$ for displacement-controlled tests, and $\log C=-11.9$ for load-controlled tests and they agree quite well as can be seen from **Fig. 11.** Further, these $\log C$ values are in good agreement with Kitagawa and Misumi's equation. Yokobori and Aizawa[7] gave theoretical basis for Kitagawa and Misumi's equation.

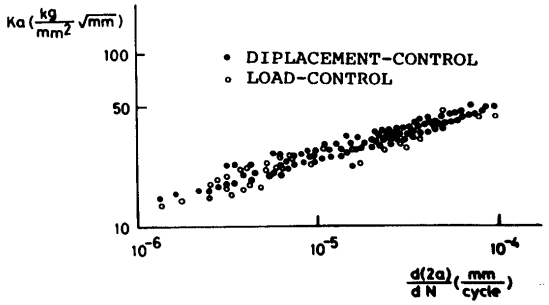

Fig. 11 Comparison of displacement-control and load-control results of sine wave load tests

In the case of random loading, the power of K in the stable crack growth region (the slope region in the $d/(2a)/dN \sim K$ curve) is $n=3.9$ for random load A, $n=3.3$ for random load B and $n=3$ for random load C. Thus, considering all the data together, i.e., the data of the displacement-controlled tests and load-controlled tests together, it is observed that as the bandwidth increases, the n value has a tendency to shift to 3. But the scatter of data is quite large and no appreciable effect of power spectra can be observed (**Fig. 12**).

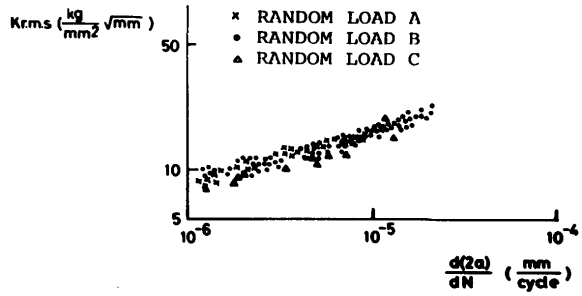

Fig. 12 Fatigue crack growth under random loading

Comparing the K_{th} values of sine wave load and random load, the following relation can be roughly observed.

$$\frac{(K_a)_{th}}{(K_{rms})_{th}} \fallingdotseq \frac{\sigma_{clip}}{\sigma_{rms}} = \text{clipping ratio}$$

where σ_{clip} is the maximum stress determined by the level of the protective limiter device in the electronic circuits. From this relation, it is considered that in the case of random loading, at the low K level, crack grows only by high peak stresses and crack growth rate becomes exceedingly slow if the K value of these peak stresses fall below $(K_a)_{th}$ level. As the random loads applied in this investigation are comparatively narrow in bandwidth, isolated peak stresses are rarely to be seen. Therefore, the frequency of high peak stresses is fairly high in the present case, so that further examination is needed whether this relation holds for such random loads with exceedingly small frequency of peak stresses.

If we compare the sine wave load data and random load data in the stable crack growth region, the log C value is greater under random load, and thus crack growth rate is seemingly faster under random loading, if the stress intensity factors are expressed in terms of K_a for sine wave load, and K_{rms} for random load. If we compare the random load data with sine wave load data by multiplying the rms value by $\sqrt{2}$ as is often performed in the electronics, the random load data is approximately 17% higher in the log C value.

5. Application to Weldments

The application of the above obtained results to weldments will be considered.

It should be noted that the relation $d(2a)/dN=CK^n$ was obtained for Stage II fatigue crack propagation. And it is generally accepted that fatigue crack propagation in this region is quite insensitive to the material's microstructure. Therefore, although the above experimental results were obtained on base metal alone, they are expected to provide information on Stage II crack growth in weldments. In fact, Koshiga and Kawahara[8] investigated fatigue crack growth in SM41, SM50, HT60, and HT80 and showed that there is no difference in fatigue crack growth rate between base metal, weld metal and HAZ. i.e., fatigue crack growth in Stage II is not influenced by the difference of the welding thermal cycles the specimens are subjected to. It should also be noted that the crack-susceptible part of the welded joint is often subjected to quite high cyclic strain, so that a crack is expected to begin to propagate by the plastic process immediately after initiation. The experimental relations of $d(2a)/dN=CK^n$ in steels under random loading will, therefore, serve as design curves to avoid fatigue failures in welded structures.

6. Summary

The following two series of tests were conducted in this investigation in order to clarify fatigue crack growth in steels under random loading.

The displacement-controlled uni-axial fully reversed tension-compression tests were conducted utilizing the bending of a composite beam, and sine wave load and two random loads with different power spectra were applied to S20C-equivalent cold rolled thin steel sheet specimen.

The load-controlled uni-axial fully reversed tension-compression tests were also performed, and sine wave load and random load of another kind were applied to S35C-equivalent steel sheet specimen.

The following conclusions were reached by analyzing the data based on linear fracture mechanics.

(1) In the sine wave load tests, fatigue crack growth rate can be expressed in the following form in the stable crack growth region both under displacement-controlled and load-controlled tests.

$$d(2a)/dN=CK_a^4$$

where K_a denotes the stress intensity factor with its stress expressed in amplitudes; $K_a=\sigma_a\sqrt{\pi a}$, and C was obtained as $C=7.78\times10^{-12}$ under displacement-con-

trolled tests and $C=6.38\times10^{-12}$ under load-controlled tests. Both results agree quite well because their log C values differ only by less than 1%.

(2) In the random load tests, fatigue crack propagation rate can also be expressed in the stable crack growth region in the following form,

$$d(2a)/dN=CK_{rms}^{n}$$

where K_{rms} denotes the stress intensity factor with its stress expressed in the instantaneous rms stress value; $K_{rms}=\sigma_{rms}\sqrt{\pi a}$. The exponent n of K shows a tendency to approach from 3 to 4 with the increase of bandwidth in random loading. But no appreciable effect of power spectra on C and n can be observed if its scatter is considered.

(3) The threshold for fatigue crack growth, K_{th}, was obtained both under sine wave loading and under random loading. The K_{th} value under sine wave loading is $(K_a)_{th}=12$ kg/mm$^2\sqrt{\text{mm}}$ for S20C-equivalent cold rolled steel and $(K_a)_{th}=12$ kg/mm$^2\sqrt{\text{mm}}$ for S35C-equivalent steel. The K_{th} under random loading was related to the K_{th} under sine wave loading, for the range of this investigation, in the following form,

$$(K_a)_{th}/(K_{rms})_{th}=\text{clipping ratio}$$

(4) The experimental relations of $d(2a)/dN=CK^n$ in steels under random loading presented in this paper will serve as design curves and will provide information on Stage II fatigue crack propagation in weldments.

Acknowledgement

The author gratefully acknowledges the encouragement and discussion he received from Prof. Hiroyuki Okamura, University of Tokyo and Dr. Koji Koibuchi, Hitachi, Ltd.

References

1) Y. Naito and H. Okamura, "Fatigue Crack Propagation under Program Loads", 1975 JSME-ASME Appl. Mech. Western Conf., p. 65
2) H. Okamura et al, "Applications of the Compliance Concept in Fracture Mechanics", ASTM STP 536, (1973–8), p. 423
3) O. L. Bowie, "Symmetric Edge Crack in Tensile Sheet with Constrained Ends", Trans. ASME, Ser. E, Vol. 31, No. 4 (1964–12), p. 726
4) O. L. Bowie, "Rectangular Tensile Sheet with Symmetric Edge Cracks", Trans. ASME, Ser. E, Vol. 31, No. 2, (1964–6), p. 208.
5) H. Kitagawa and M. Misumi, "Estimation of Effective Stress Intensity Factor for Fatigue Crack Growth Considering the Mean Stress", Proc. ICM-I, SMSJ, (1972), p. 225
6) T. Yokobori and T. Aizawa, "Some Notes to the Kinetic Theory of Fatigue Crack Propagation Rate", Rep. Res. Inst. Strength of Materials, Tohoku Univ. Vol. 9, No. 2 (1973–12), p. 65
7) F. Koshiga and M. Kawahara, "A Proposed Design Basis with Special Reference to Fatigue Crack Propagation", Journal of Soc. Naval Arch. Japan, Vol. 133, p. 249 (inJapanese)